Physics Letters A 383 (2019) 2640–2644

Contents lists available at ScienceDirect

Physics Letters A

www.elsevier.com/locate/pla

Phase modulation of acoustic vortex beam with metasurfaces

Jun-Feng Zeng [a], Xin Zhang [b,*], Fu-Gen Wu [a,*], Li-Xiang Han [a], Qiang Wang [a], Zhong-Fei Mu [c], Hua-Feng Dong [b], Yuan-Wei Yao [b]

[a] School of Materials and Energy, Guangdong University of Technology, Guangzhou 510006, China
[b] School of Physics and Optoelectronic Engineering, Guangdong University of Technology, Guangzhou 510006, China
[c] School of Experiment Education, Guangdong University of Technology, Guangzhou 510006, China

ARTICLE INFO

Article history:
Received 5 November 2018
Accepted 14 May 2019
Available online 17 May 2019
Communicated by R. Wu

Keywords:
Acoustic metasurface
Acoustic vortex beam
Phase modulation

ABSTRACT

We present a new acoustic metasurface structure to generate the stable acoustic vortex beams with controllable topological charge in the broadening of operating frequency. The proposed acoustic metasurface can dynamically achieve a full span of 360° phase modulation by three simple solutions. Acoustic plane beam and acoustic vortex beam can convert each other based on multi-metasurfaces combination. Potential applications of such phase modulation schemes can be anticipated.

1. Introduction

Acoustic metasurfaces, [1–6] the planarized version of metamaterials with a subwavelength thickness, have attracted tremendous attention in recent years due to their excellent properties in manipulating the acoustic beam fronts and phase. [7–16] Many efforts have been made by employing these metasurfaces, such as acoustic communication [17], acoustic spanner [18,19], acoustic vortex generator [20–24]. Acoustic vortex beams, features by a screwing phase dislocation, have been successfully applied in many places such as acoustic tweezers, [25] wave computations, [26] and acoustic alignment. [27] Traditionally, the phase modulations are achieved by modulating the refractive index of non-subwavelength materials which are too bulky for acoustic integration. Currently available metasurface-based phase modulators are mostly passive elements, which cannot dynamically modulate the phase of acoustic vortex beams.

In this paper, we systematically study the strategies of phase modulation and drastically modulate the phase of the acoustic vortex beams, using full-wave simulations. Throughout the paper, all full-wave simulations are performed by the commercial finite-element simulation software (COMSOL Multiphysics). We design a simple metasurface with a subwavelength thickness to generate the stable acoustic vortex beams. Based on the metasurface, effective schemes are proposed to achieve a full span of 360° dynamic phase modulation of the acoustic vortex beams. The proposed methods suggest new design strategies for future active phase modulators of acoustic vortex beams.

1.1. Structure and results

We utilize Helmholtz resonators as the building block to construct the planar layer as an assembly of six fanlike sections over the whole azimuth. Fig. 1(a) shows the sectional view of the assembled layer. The six fanlike sections gives a reasonably good resolution for generating a stable vortex beam with a topological charge $m = 1$, as will be demonstrated via numerical simulations. Fig. 1(b) demonstrates the supercell composed by six subunits. The first individual section is configured to be composed of one column of resonator in the radius. Each column consists of one Helmholtz cavity and one fanlike thin plate locating in the central location. The other individual sections are made by increasing the number of the column and changing the width of the import and export of the first individual section. Calculated phase of six subunits with a near-linear phase gradient of nearly 60 degrees cover the full range of 360 degrees, shown in Fig. 1(c). The metasurface is designed to operate in air with the sound frequency of 0.5 MHz and the subunit is made of copper. The Helmholtz resonator-like structures provide a high transmission property of the acoustic beam and a discrete phase gradient required for the 360 degrees range of the acoustic metasurface. Each individual fanlike section has the same thickness $l = 0.6\lambda$ and radial $h = 0.48\lambda$. The combination of cavities and plates provides hybrid resonances to overcome the

* Corresponding authors.
E-mail addresses: xinxintwinkle@163.com (X. Zhang), Wufg@gdut.edu.cn (F.-G. Wu).

https://doi.org/10.1016/j.physleta.2019.05.027
0375-9601/

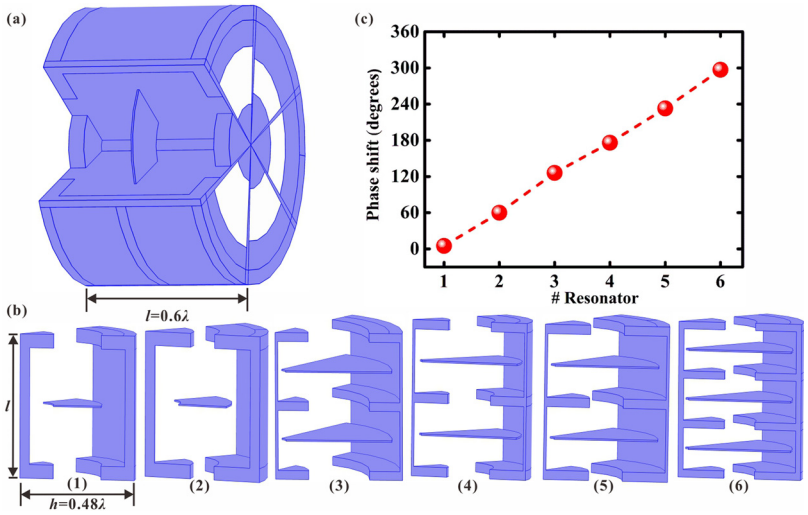

Fig. 1. A simple structure consisting of copper to realize the transmitted acoustic gradient metasurface. (a) Schematic demonstration of the assembled layer consisted of six fanlike sections of resonators (the thickness $l = 0.6\lambda$ with λ being the sound wavelength). (b) Each individual fanlike section consisting of large fanlike cavities connected by fanlike flats with the same number (the radial resolution $h = 0.48\lambda$), sided by flats of varying the width of the import and export of resonator to produce the desired phase. (c) Numerically optimized phase (red solid circles) for the six fanlike resonators. (For interpretation of the colors in the figure(s), the reader is referred to the web version of this article.)

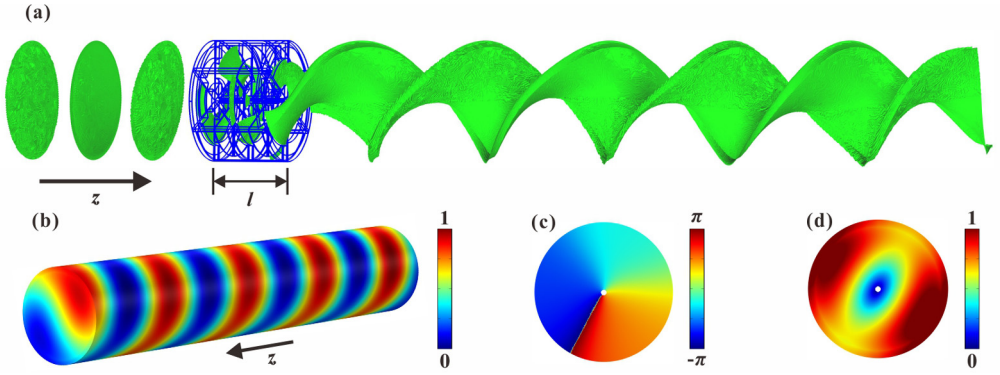

Fig. 2. The characteristics of the acoustic vortex beam. (a) The resonant layer (blue line area) converting an in-coming axisymmetric wave without orbital angular momentum (OAM) to an outgoing beam with a helical wave front carrying OAM (wave fronts are shown in green). (b) The simulated total acoustic pressure field on the outgoing surface of the planar layer (located at $0 \le z \le 5.4\lambda$) and the inner surface of cylindrical waveguide of 0.48λ radius. (c) Measured phase distributions (top) and (d) amplitude (bottom) of acoustic vortex beam, where the geometric centers of the cross section are denoted by the while dots. The simulations are for sound of a frequency 0.5 MHz ($\lambda = 0.68$ mm in air).

impedance mismatch between the resonators and the surrounding air for a high transmission.

In order to generate higher-order vortex beams, the number of sections in the matesurface can be increased for an efficient resolution. The series connection of cavities and plates acting as lumped elements is for a fully flexible manipulation of acoustic wave fronts and phase.

By full-wave simulation, the resonant layer successfully converts an in-coming axisymmetric wave without OAM to an outgoing beam with a helical wave front carrying OAM, shown in Fig. 2(a). In Fig. 2(b), the simulated total acoustic pressure field through the whole metasurface clearly shows an expected twisted wave front with a screw dislocation along the propagation axis. The distribution of phases at the cross sections represents the characteristic of the acoustic vortex beam and illustrates the expected topological charge $m = 1$, shown in Fig. 2(c). Another representative characteristic of the acoustic vortex beam is the null pressure amplitude at the core, shown in Fig. 2(d).

1.2. Frequency broadening effect

Fig. 3(a) shows the acoustic transmission spectrum of the metasurface filling with air. The structures of the metasurface are fixed at $l = 0.68$ mm. It can be seen that are three transmission peaks with a certain width for generating vortex beam from 0.430 MHz to 0.525 MHz. The transmittance is greater than 90% in a band of frequencies ranging from 0.451 MHz to 0.453 MHz and 0.502 MHz to 0.503 MHz. That is to say, in the case of the fixed structure of the metasurface, it still maintains a high transmission ability to the sound wave in certain frequency range to generate sound vortices by metasurface. In the frequency range of 0.430 MHz-0.525 MHz, the metasurface is feasible to control the transmitted acoustic wave to generate acoustic vortex beams.

The simulated transmission through the whole layer (via three-dimensional simulations in the air-filled waveguide) generates vortex beams fronts along the propagation axis shown in Fig. 3(b). These vortex wave fronts are generated with different topological charge in different incident wave frequency. As the incident wave frequency increases, the number of the topological charge of the vortex beams also increases.

1.3. Phase distributions modulation of acoustic vortices

The thickness of the metasurface is fixed at $l = 0.6\lambda$ and the working frequency of the incident acoustic plane beam is 0.5 MHz. All simulations are performed at the same standard atmospheric

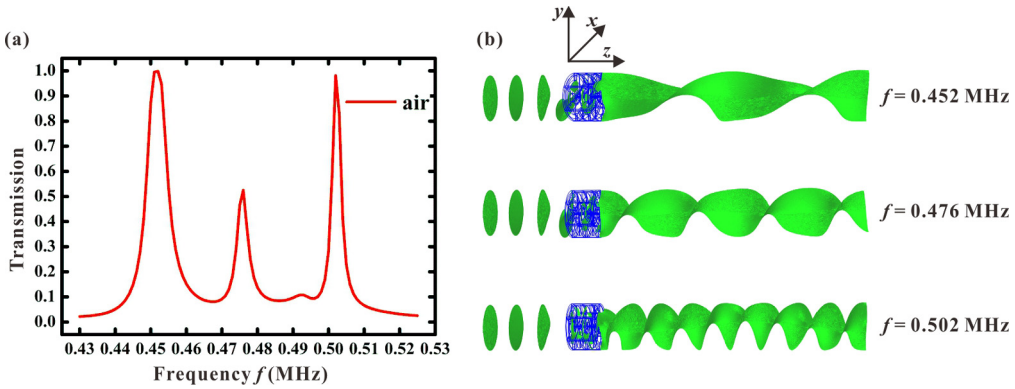

Fig. 3. The frequency broadening effect of the proposed acoustic metasurface filling with gas of air (0 °C). (a) The transmission of the metasurface filling with air (0 °C) under the planar incident wave as functions of the incident frequency. The vortex beams can be generated within this frequency ranges. (b) The metasurface can generate vortex beams with different topological charge m for the normally incident wave of 0.452 MHz, 0.476 MHz and 0.502 MHz. The wave front of different incident frequency at the same distance is away from the designed structure.

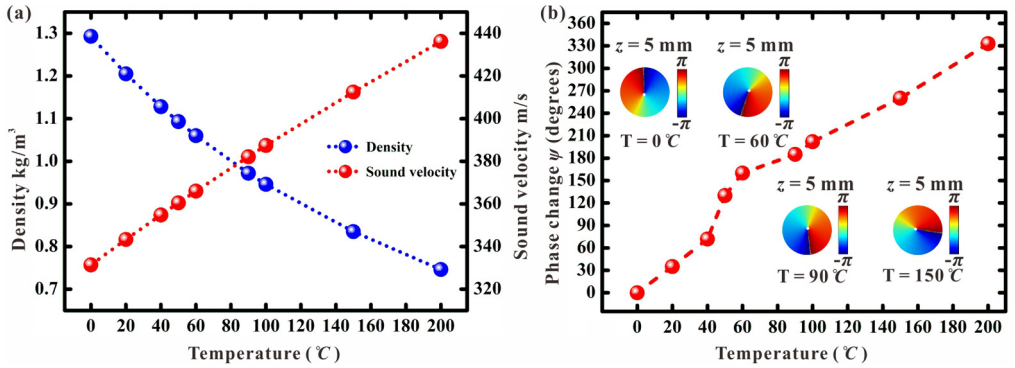

Fig. 4. The parameters of air at different temperatures and the phase distributions modulation of acoustic vortices by changing the temperature of the filling air. (a) The values of density and sound velocity of air filled in metasurface as functions of different temperatures. (b) Simulated and measured relationships between temperature variation and the phase variation. Inset: summary of the schematic of the 0 °C, 60 °C, 90 °C and 150 °C of the filling air of the metasurface, simulated phase distributions in 0.5 MHz at the cross-section $z = 5$ mm.

pressure p = 101.325 kPa. As can be seen in the Fig. 4(a), blue solid circles and red solid circles represent the density and sound velocity of air filled in one metasurface at nine different temperatures, respectively. The phase modulation of acoustic vortex beams can be achieved by changing the temperature of the filling air. A summary of the simulated phase distribution (normalized with the corresponding maximums) of the 0 °C to 200 °C in 0.5 MHz at the cross-sections z = 5 mm are illustrated in Fig. 4(b). It can be observed that the phases have changed 0, 160, 185 and 333 degrees counterclockwise in an annular loop of the diffraction phase fields generated by identical metasurfaces dilled with identical air at different temperatures. So we can dynamically modulate the phase of the acoustic vortex beams by changing the temperature of the filling air.

The working frequency of the incident acoustic plane beams is fixed at 0.5 MHz. Equiphase surfaces of pressure along the propagation axis for the first order vortex beam generated by two identical metasurfaces which are sequentially placed and filled with gas of air (0 °C). The acoustic beams with different topological charge m of left 0, center 1 and right −1, propagate in waveguide filled with air Fig. 5(a). Fig. 5(b) shows the phase distributions measured at the right side of the right hand side metasurface $z = 5$ mm and regards the phase distributions ψ as 0 degrees artificially. Only rotating the right metasurface by $\theta = 30$ degrees on z axis clockwise, the angles of the equiphase surface of pressure rotate on z axis clockwise Fig. 5(c). Phase distributions measured at the same place as Fig. 5(b), the phase profile is measured to rotate an angle of $\psi = 60$ degrees between Fig. 5(b) and Fig. 5(d). Rotating the right hand side metasurface by different angle θ on z axis clockwise, the phase distributions ψ changed with θ. The range of θ is from 0 to 360 degrees. The phase distribution ψ have shifted from 0 to 320 degrees for one time in the air-filled waveguide Fig. 5(e).

We modulate the phase of transmission acoustic vortex beam by filling the left hand side metasurface with gas of CO_2 (0 °C) and filling the right hand side metasurface with another gas (0 °C). Two identical metasurfaces are sequentially placed and the distance between them is 9λ. The thickness of the metasurface is fixed at $l = 0.6\lambda$ and all simulations are performed at the same standard atmospheric pressure p = 101.325 kPa. As can be seen in the Fig. 6(a), blue solid circles and red solid circles represent the density and sound velocity of different gases filled in the right hand side metasurface at identical temperature, respectively. Fig. 6(b) shows the value of phase distributions ψ (red solid circles) changed with nine different types of gases (0 °C), which are individually filled in the right hand side metasurface. The phase distributions measured at the right side of the right hand side metasurface $z = 5$ mm. It can be observed that the phase have changed 0, 135, 305 and 353 degrees by filling the right hand side metasurfaces with gas of NO, NO_2, CO, N_2 (0 °C), where the geometric centers of the cross sections are denoted by while dots. The abilities of these gases to modulate the phase of acoustic vortices are gradient increase. We use metasurfaces to modulate spiral phases distribution of acoustic vortex based on the gas combination. A full span of 360 degrees phase modulation can be achieved by filling the two identical metasurfaces with two different types of gases. The gases combination scheme provides an effective and compact solution to generate counterclockwise acous-

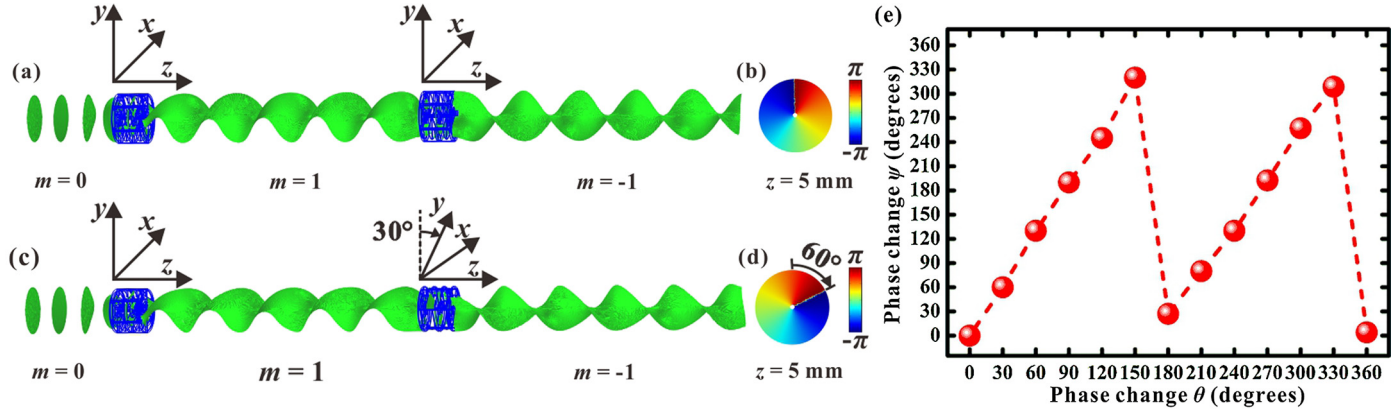

Fig. 5. Phase distributions modulation of acoustic vortices by two identical metasurfaces. (a) Generating acoustic vortex beams base with OAM topological charges −1 to 1 in the air-filled waveguide. (b) Measured phase distributions of acoustic vortex beam at the right hand side of the right hand side metasurface $z = 5$ mm. (c) Only rotating the right metasurface by $\theta = 30$ degrees clockwise, the equiphase surface of pressure changed. (d) Measured phase distributions of acoustic vortex beam at the same place as (b). The phase distribution has shifted by 60 degrees clockwise compared with (b). (e) Only rotating the right hand side of metasurface by different θ clockwise, the phase distributions ψ changed with θ.

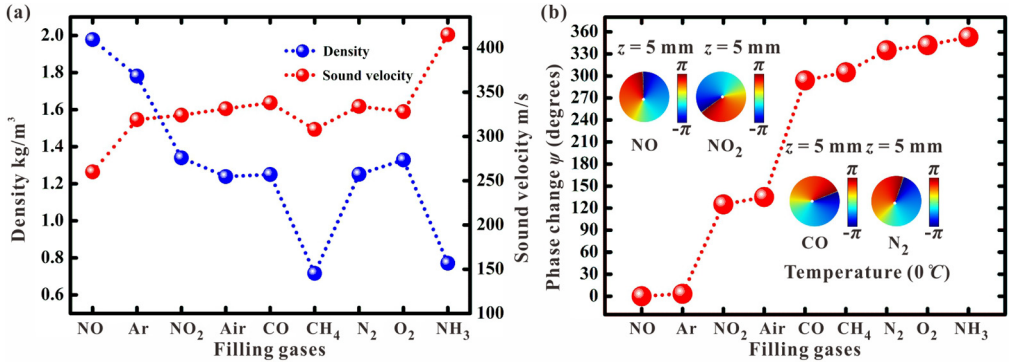

Fig. 6. Phase distributions modulation of acoustic vortices by filling two identical metasurfaces with different types of gases (0 °C). (a) The parameters of different filling gases at identical temperature of 0 °C. (b) Phase distributions measured at the right hand side of the right hand side metasurface $z = 5$ mm. Simulated and measured relationships between gas variation and the phase variation.

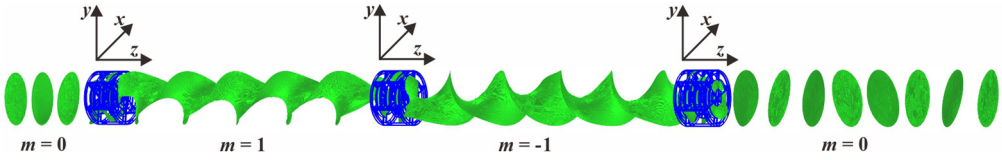

Fig. 7. Modulating the acoustic vortex beam to the acoustic plane beams by three identical metasurfaces.

tic vortex beam and clockwise acoustic vortex beam at the same time.

1.4. Transformation between vortex beam and plane beam

As can be seen in the Fig. 7, we propose a simple method to modulate the equiphase surfaces of pressure of acoustic vortices by three identical metasurfaces, which are sequentially placed and the distance between adjacent metasurfaces are all 5.4λ. The working frequency of the incident acoustic plane beams is fixed at 0.384 MHz. The three identical metasurfaces are all immersed in the air-filled waveguide, in which the temperature of air is 0 °C. It can be observed that the topological charge of the acoustic wave are $m = 0$, $m = 1$, $m = -1$ and $m = 0$ along the propagation axis. We produce the acoustic vortex beams that can rotate on z axis clockwise ($m = 1$) and also can rotate on z axis counterclockwise ($m = -1$) at the same time. Finally we convert the acoustic vortex beam to the acoustic plane beams ($m = 0$) by the method of combining three identical metasurfaces. This scheme provides a simple and effective solution to convert the acoustic vortex beam to the acoustic plane beams, which can advance the capability of modulating phase distribution for further applications of the acoustic vortex beams.

2. Conclusions

In summary, we propose a new and simple design of a transmitted acoustic metasurface to generate the stable acoustic vortices with high transmittance efficiency. The proposed metasurface can not only convert between acoustic vortex beams and acoustic plane beams, but also can dynamically modulate the phase of the vortex beams by changing the temperature of the filling air, rotating the angle of the metasurface or changing the combined type of the filling gases. Another interesting property is that the proposed metasurface can generate vortex beams with different topological charge in the broadening of operating frequency. The schemes of generating acoustic vortex beam, dynamically modulating the phase and converting acoustic vortex beam to acoustic plane beams provide potential applications in information transmission and acoustic transducer.

Acknowledgements

This work was supported by the National Natural Science Foundation of China under Grant Nos. 11374066, 11374068 and 11674310, the Natural Science Foundation of Guangdong Province under Grant No. S2012020010885 and Guangdong University of Technology Graduate Innovation Project under Grant No. 262523667.

References

[1] Y. Li, B. Liang, Z.-M. Gu, X.-Y. Zou, J.-C. Cheng, Reflected wavefront manipulation based on ultrathin planar acoustic metasurfaces, Sci. Rep. 3 (2013) 2546, https://doi.org/10.1038/srep02546.

[2] Y. Li, X. Jiang, R.-Q. Li, B. Liang, X.-Y. Zou, L.-L. Yin, J.-C. Cheng, Experimental realization of full control of reflected waves with subwavelength acoustic metasurfaces, Phys. Rev. Appl. 2 (2014) 064002, https://doi.org/10.1103/PhysRevApplied.2.064002.

[3] K. Tang, C.-Y. Qiu, M.-Z. Ke, J.-Y. Lu, Y.-T. Ye, Z.-Y. Liu, Anomalous refraction of airborne sound through ultrathin metasurfaces, Sci. Rep. 4 (2014) 6517, https://doi.org/10.1038/srep06517.

[4] Y.-B. Xie, W.-Q. Wang, H.-Y. Chen, A. Konneker, B.-I. Popa, S.-A. Cummer, Wavefront modulation and subwavelength diffractive acoustics with an acoustic metasurface, Nat. Commun. 5 (2014) 5553, https://doi.org/10.1038/ncomms6553.

[5] J. Mei, Y. Wu, Controllable transmission and total reflection through an impedance-matched acoustic metasurface, New J. Phys. 16 (2014) 123007, https://doi.org/10.1088/1367-2630/16/12/123007.

[6] K. Tang, C.-Y. Qiu, J.-Y. Lu, M.-Z. Ke, Z.-Y. Liu, Focusing and directional beaming effects of airborne sound through a planar lens with zigzag slits, J. Appl. Phys. 117 (2015) 024503, https://doi.org/10.1063/1.4905910.

[7] A. Grbic, L. Jiang, R. Merlin, Near-field plates: subdiffraction focusing with patterned surfaces, Science 320 (2008) 511–513, https://doi.org/10.1126/science.1154753.

[8] N.-F. Yu, P. Genevet, M.-A. Kats, F. Aieta, J.-P. Tetienne, et al., Light propagation with phase discontinuities: generalized laws of reflection and refraction, Science 334 (2011) 333–337, https://doi.org/10.1126/science.1210713.

[9] P.-Y. Chen, A. Alù, Mantle cloaking using thin patterned metasurfaces, Phys. Rev. B 84 (2011) 205110, https://doi.org/10.1103/PhysRevB.84.205110.

[10] X.-J. Ni, N.-K. Emani, A.-V. Kildishev, A. Boltasseva, V.-M. Shalaev, Broadband light bending with plasmonic nanoantennas, Science 335 (2012) 427, https://doi.org/10.1126/science.1214686.

[11] J. Lin, J.P.-B. Mueller, Q. Wang, G.-H. Yuan, N. Antoniou, et al., Polarization-controlled tunable directional coupling of surface plasmon polaritons, Science 340 (2013) 331–334, https://doi.org/10.1126/science.1233746.

[12] C. Pfeiffer, A. Grbic, Metamaterial Huygens' surfaces: tailoring wave fronts with reflectionless sheets, Phys. Rev. Lett. 110 (2013) 197401, https://doi.org/10.1103/PhysRevLett.110.197401.

[13] F. Monticone, N.-M. Estakhri, A. Alù, Full control of nanoscale optical transmission with a composite metascreen, Phys. Rev. Lett. 110 (2013) 203903, https://doi.org/10.1103/PhysRevLett.110.203903.

[14] A.-D. Rubio, D. Torrent, J. Carbonell, J.-S. Dehesa, Extraordinary absorption by a thin dielectric slab backed with a metasurface, Phys. Rev. B 89 (2014) 245123, https://doi.org/10.1103/PhysRevB.89.245123.

[15] W.-Q. Zhang, X. Zhang, F.-G. Wu, Y.-W. Yao, S.-F. Lua, H.-F. Dong, Z.-F. Mu, J.-b. Li, Angular control of acoustic waves oblique incidence by phononic crystals based on Dirac cones at the Brillouin zone boundary, Mod. Phys. Lett. A 382 (2018) 423–427, https://doi.org/10.1016/j.physleta.2017.12.014.

[16] L.-X. Han, Y.-W. Yao, X. Zhang, F.-G. Wu, H.-F. Dong, Z.-F. Mu, J.-b. Li, Acoustic metasurface for refracted wave manipulation, Mod. Phys. Lett. A 382 (2018) 357–361, https://doi.org/10.1016/j.physleta.2017.12.004.

[17] C.-Z. Shi, M. Duboisa, Y. Wang, X. Zhang, High-speed acoustic communication by multiplexing orbital angular momentum, Proc. Natl. Acad. Sci. 114 (2017) 7250, https://doi.org/10.1073/pnas.1704450114.

[18] K.-D. Skeldon, C. Wilson, M. Edgar, M.-J. Padgett, An acoustic spanner and its associated rotational Doppler shift, New J. Phys. 10 (2008) 013018, https://doi.org/10.1088/1367-2630/10/1/013018.

[19] K.-V. Sepulveda, A.-O. Santillan, R.-R. Boullosa, Transfer of angular momentum to matter from acoustical vortices in free space, Phys. Rev. Lett. 100 (2008) 024302, https://doi.org/10.1103/PhysRevLett.100.024302.

[20] J.-L. Ealo, J.-C. Prieto, F. Seco, Airborne ultrasonic vortex generation using flexible ferroelectrets, IEEE Trans. Ultrason. Ferroelectr. Freq. Control 58 (2011) 1651, https://doi.org/10.1109/TUFFC.2011.1992.

[21] L.-P. Ye, C.-Y. Qiu, J.-Y. Lu, K. Tang, H. Jia, M.-Z. Ke, S.-S. Peng, Z.-Y. Liu, Making sound vortices by metasurfaces, AIP Adv. 6 (2016) 085007, https://doi.org/10.1063/1.4961062.

[22] X. Jiang, Y. Li, B. Liang, J.-C. Cheng, L.-K. Zhang, Convert acoustic resonances to orbital angular momentum, Phys. Rev. Lett. 117 (2016) 034301, https://doi.org/10.1103/PhysRevLett.117.034301.

[23] X. Jiang, J.-J. Zhao, S.-L. Liu, B. Liang, X.-Y. Zou, J. Yang, C.-W. Qiu, J.-C. Cheng, Broadband and stable acoustic vortex emitter with multi-arm coiling slits, Appl. Phys. Lett. 108 (2016) 203501, https://doi.org/10.1063/1.4949337.

[24] Y.-R. Jia, Q. Wei, D.-J. Wu, Z. Xu, X.-J. Liu, Generation of fractional acoustic vortex with a discrete Archimedean spiral structure plate, Appl. Phys. Lett. 112 (2018) 173501, https://doi.org/10.1063/1.5026646.

[25] F. Guo, Z.-M. Mao, Y.-C. Chen, Z.-W. Xie, J.-P. Lata, P. Li, L.-Q. Ren, J.-Y. Liu, J. Yang, M. Dao, S. Suresh, T.-J. Huang, Three-dimensional manipulation of single cells using surface acoustic waves, Proc. Natl. Acad. Sci. 113 (2016) 1522, https://doi.org/10.1073/pnas.1524813113.

[26] R. Marchiano, J.-L. Thomas, Doing arithmetic with nonlinear acoustic vortices, Phys. Rev. Lett. 101 (2008) 064301, https://doi.org/10.1103/PhysRevLett.101.064301.

[27] B.-T. Henfner, P.-L. Marston, An acoustical helicoidal wave transducer with applications for the alignment of ultrasonic and underwater systems, J. Acoust. Soc. Am. 106 (1999) 3313, https://doi.org/10.1121/1.428184.